Probing the electronic nature of Co centers forming the planar ring in octa-nuclear Co complexes using X-ray absorption spectroscopy

Nirupamjit Sarmah[1], Deepa Sharma[2], B.K.Mehta[2], B.D.Shrivastava[3], B.K.Das[1], A. Zimina[4,5], A.Gaur[4,5*]

[1]*Department of Chemistry, Gauhati University, Guwahati 781 014, India*
[2]*School of Studies in Chemistry and Bio-chemistry, Vikram University, Ujjain 456010, India*
[3]*School of Studies in Physics, Vikram University, Ujjain 456010, India*
[4]*Institute of Catalysis Research and Technology (IKFT), Karlsruhe Institute of Technology, Eggenstein-Leopoldshafen 76344, Germany*
[5]*Institute for Chemical Technology and Polymer Chemistry (ITCP), Karlsruhe Institute of Technology, Karlsruhe 76131, Germany*

**Corresponding author:* abhijeet.gaur@kit.edu, abhijeetgaur9@gmail.com

Abstract

The formation of octanuclear cobalt core has been studied in the Co complexes $Na[Co_8\{O_2CCH_3\}_8(OCH_3)_{16}]NO_3$(**1**), $Na[Co_8\{O_2CC(CH_3)_3\}_8(OCH_3)_{16}]NO_3$(**2**), $Na[Co_8\{O_2CC(CH_3)_3\}_8(OC_2H_5)_{16}]NO_3$(**3**) by analysing the X-ray absorption spectra at the Co K-edge. Analysis of EXAFS confirmed octahedral coordination around the Co atoms. The presence of neighbouring Co atoms has been associated to the octanuclear nature of the complexes. The XANES features have been correlated with the oxidation state of the absorbing Co atoms and their coordination in the complexes. XANES spectra have been simulated by ab-initio XANES calculations performed for the Co centres forming the planar ring in order to investigate and compare the electronic nature of these metal centres. Co density of states (DOS), i.e., s-, p- and d-DOS have also been calculated to explain the different features of XANES spectra. The simulated XANES spectra are further compared with the experimental spectra to probe the effect of different ligands present in the complexes.

Keywords – *Octa-nuclear cobalt complexes; X-ray absorption fine structure; Ab initio XANES calculations; density of states*

Co centers forming a planar ring in octa-nuclear Co complexes

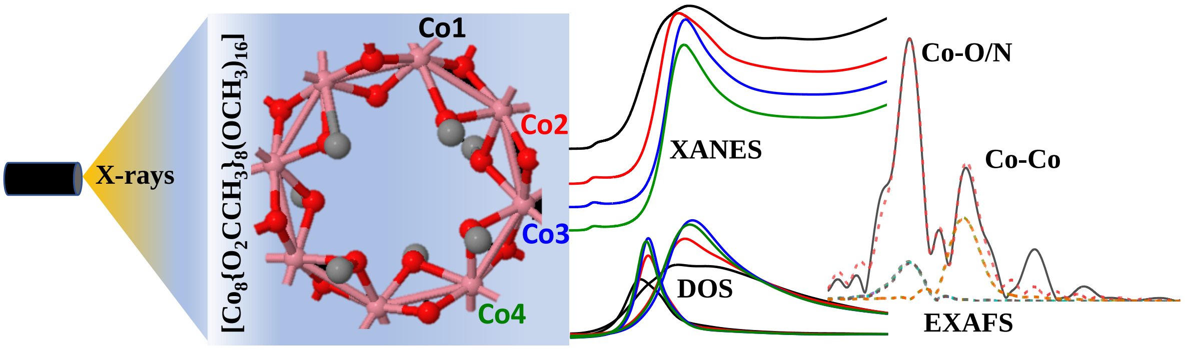

1. Introduction

High-nuclearity oxide-bridged 3d metal carboxylate complexes are known to display interesting structural, spectroscopic and magnetic properties[1]. Cobalt carboxylates have proved to be useful as homogenous catalysts in industry, noticeably in the oxidation of *p*-xylene, methyl benzenes, ethanol, butane, acetaldehyde etc[2]. Several Co^{3+} cubane like complexes have been synthesized and used as homogeneous as well as heterogeneous catalysts.[3] The structure of the symmetric cubane consists of an appropriate cube having four Co^{3+} and four O^{2-} ions at the alternate corners. The cubane forms the core of the complexes of the type $Co_4O_4(O_2CR)L_4$ [L=py or a 4-substituted pyridine and R= aryl or methyl group]. In the present investigation we are concerned with molecular species having $[Co_8(\mu_4\text{-}O)_4]$ core[4]. The structure of these octanuclear Co complexes contains $[Co_8O_4]^{12+}$ core consisting of the inner cubane $[Co_4O_4]$, with the additional four Co atoms bonded to the oxygen atoms. While, the Co atoms forming the cubane core have trigonal pyramidal geometry, the Co atoms forming the octagon have distorted octahedral geometry. The initial examples of such complexes are $[Co_8O_4(O_2CPh)_{12}(Solv)_4]$ (where Solv=MeCN, DMF, H_2O), which were synthesized and characterized by Dimitrou et. al.[4]

Beattie et al.[5] isolated the octanuclear cobalt complexes $[Co_8(O)_4(OAc)_6(OMe)_4Cl_4(OH_n)_4].6H_2O$, (n=1,2) following recrystallisation of the products of reaction of $[Co(OAc)_2].4H_2O$ with acetic acid and ozone. The structural motif of this octanuclear complex differs from that prepared by Dimitrou et. al[6]. It is found to contain a central $[Co_8O_8]$ core formed by a linear array of face-sharing three $[Co_4O_4]$ cubane fragments. In another study, Beattie et. al[7] isolated and synthesized octanuclear material $[NH_4][Co_8(MeCO_2)_8(OMe)_{16}][PF_6]$. X-ray crystallography showed that it consists of a molecule of $[Co_8(MeCO_2)_8(OMe)_{16}]$ having highly symmetric toroidal shape with the NH_4^+ ion situated at the centre. The toroidal shape contains four $[Co_2(\mu\text{-}MeCO_2)(\mu\text{-}OMe)_2]$ units forming edge-sharing eight CoO_6 distorted octahedra. The eight Co atoms are at the vertices of a nearly regular planar octagon.

Several studies have been reported describing the unique structure of the Co multinuclear complexes and their magnetic properties. Brechin et. al[8] have synthesized and characterized dodecanuclear cobalt wheels complex $[Co_{12}(chp)_{12}(O_2CMe)_{12}(H_2O)_6(Thf)_6]$ (where chp = 6-chloro-2-pyridonate and Thf = tetrahydrofuran) and studied its magnetic properties. Furusova et. al[9] synthesized and characterized four hexanuclear, one octanuclear, three nonanuclear and two decanuclear cobalt complexes. Lapshin and Magdysyuk al[10] isolated a octanuclear mixed valence cobalt complex. $[Co_4^{2+}Co_4^{3+}(\mu_4\text{-}O)_4(\mu\text{-}O_2CPh)_{12}(C_2H_5OH)_4\cdot 3C_3H_6O\cdot C_2H_5OH$ (Ph = phenyl, C_6H_5), which has chelate open cavities. The complex involves a rare core $[Co_8O_4]^{12+}$ consisting of the cubane $[Co_4^{3+}O_4]^{4+}$ having oxygen atoms bonded to the four additional Co^{2+} atoms. Russell et. al[11] have synthesized and characterized an octanuclear Co^{2+} complex $[Co_8(HL)_8(O)(OH)_4(MeOH)_3H_2O]$-$[ClO_4]_3{\cdot}5MeOH{\cdot}2H_2O$ (where HL = N-(2-pyridyl)-3-carboxypropannamide) consisting of an octanuclear Co^{2+} cluster built around a $[Co_4OH]$ square assembly. The complex shows dominant anti-ferromagnetic interaction. Holmberg et. al[12] have synthesised cubic octanuclear Co^{2+} metal organic framework (MOF) structure $[Co^{2+}{}_8(OH)_6(cpt)_6][CoCl_4]_2{\cdot}2H_2O$, (where Hept=4-(4'-carboxyphenyl)-1,2,4-trizole). Magnetic measurements and also DFT calculations show that the coupling between Co^{2+} ions in the SBU is intramolecular anti-ferromagnetic. Argent et. al[13] have synthesized nine complexes by reacting tris-carboxylic acid ligands with the metal cations of first row transition elements. The complexes were characterised by X-ray crystallography. Octanuclear mixed valent $\{Co_4^{2+}Co_4^{3+}\}$ pivalate cluster $[Co_8(O_2CCMe_3)_{10}(teaH_3)_4(N_3)](Me_3CCO_2){\cdot}MeCN{\cdot}H_2O$, $teaH_3$=triethanolamine ligand, has been synthesized along with other tetranuclear and hexanuclear cobalt clusters by Radu et. al[14]. The magnetic properties of the complex have been explained on the basis of theoretical models considering structural properties of the cluster. Alexandropoulos et. al[15] reported a unique topology among the reported Co_8 structures synthesized by self-assembly reaction between Co^{2+} metal ions and 2,2-bipyramid(bpym) neutral ligand in the presence of $[CF_3SO_3]^-$ anions. The obtained octanuclear cobalt complex $[Co_8(dbm)_8(bpm)_8](CF_3SO_3)_8$ has been shown to have weak magnetic coupling between the Co^{2+} spins.

In the present work, we have investigated the X-ray absorption fine structure (XAFS) at the K-edge of cobalt in three octanuclear cobalt complexes containing the Co_8O_4 core: $Na[Co_8\{O_2CCH_3\}_8(OCH_3)_{16}]NO_3$(**1**), $Na[Co_8\{O_2CC(CH_3)_3\}_8(OCH_3)_{16}]NO_3$(**2**) and $Na[Co_8\{O_2CC(CH_3)_3\}_8(OC_2H_5)_{16}]NO_3$(**3**). The elemental composition in these complexes have been confirmed by employing Energy Dispersive X-ray Spectroscopy (EDX) measurements. Both extended X-ray absorption fine structure (EXAFS) and X-ray absorption near edge structure (XANES) have been analysed to obtain information about local structure around the absorbing cobalt atom. Crystal structure of an complex $NH_4[Co_8\{O_2CCH_3\}_8(OCH_3)_{16}][PF_6]$(**4**) analogous to **1** is reported in literature by Beattie et. al[7]. As described, the molecules of the complexes have a highly symmetric toroidal shape formed by edge shared eight CoO_6 distorted octahedra. At the vertices of a nearly regular planar octagon are situated the cobalt atoms. The chemical sketch depicting the molecular structure of the complex **1** is shown in Fig. 1. The host molecule $[Co_8\{O_2CCH_3\}_8(OCH_3)_{16}]$ possesses a highly symmetrical toroid shape, consisting of four $[Co_2(\mu\text{-}O_2CCH_3)(OCH_3)_2]$ units, forming eight edge-shared CoO_6 distorted octahedra.

Each pair of cobalt atoms is bridged by one acetate anion and two stereochemically distinct methoxide anions, one methoxide upward and the other methoxide downward with respect to the Co_8 plane. The chemical structure of complexes **2** and **3** are similar to **1** except for the presence of different bridging ligands.

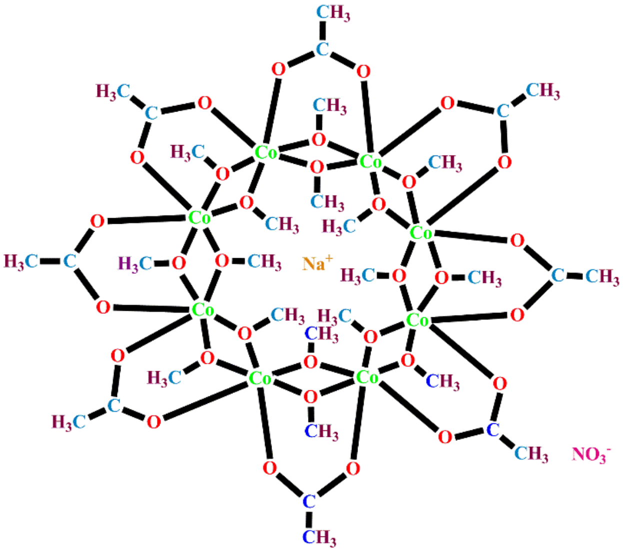

Fig 1. Chemical sketch of the octanuclear complex **1**, i.e., $[Co_8\{O_2CCH_3\}_8(OCH_3)_{16}]$.

The crystal structure of **4** has been utilized to perform EXAFS analysis in complexes **1-3** to determine the coordination environment around the Co atoms. The atoms.inp file employed in EXAFS analysis has been used further to generate feff.inp file to perform ab initio XANES simulations for each of the Co centres situated at the vertices of a octagon in order to probe their electronic nature. Corresponding Co s-, p- and d-density of states (DOS) have also been calculated and corelated to the XANES features obtained in the simulated spectra.

2. Experimental and Data analysis

2.1 Synthesis of complexes

The octanuclear complexes **1** and **3** were prepared by dissolving 5 mmol of $Co(NO_3)_2.6H_2O$ and 10 mmol of sodium pivalate in 20 mL methanol. The mixture was stirred at refluxing temperature for about 10 minutes. Then 50 mmol of 30% H_2O_2 was added gently drop wise. In the pinkish solution, green coloured ppt starts falling immediately. The mixture is stirred for 6 hrs. The ppt so obtained was filtered in suction and washed with water and methanol (for **1)**/ethanol (for **3**) and then dried in vacuum desiccator. The preparation of complex **2** was slightly different. Instead of sodium pivalate, sodium acetate was used. On addition of H_2O_2 the pinkish solution turns green in colour which is stirred for 6 hrs. The solution is then evaporated in a rotary evaporator. By adding dichloromethane, the aqueous layer separates out. On the remaining extract, petroleum ether is added to obtain a green coloured ppt. The ppt. so obtained is filtered in suction, washed and dried.

2.2 EDX

The compositional characterization of complexes **1-3** was done by EDX. For EDX measurements, an Element EDS System of EDAX-AMETEK coupled with a Zeiss Sigma 300 electron microscope was used. The APEX^{TM} software program was used for the collection and analysis of EDS data. The characteristic X-ray spectra were collected for several spots on a carefully chosen sample and the concentrations (weight% values) of the non-hydrogen elements present in the sample were typically obtained by averaging 4-5 values determined from as many spots on the sample surfaces. The weight percent values obtained from the system have been rationalized for presence of hydrogen in molecular compounds.

2.3 XAFS

XAFS was recorded at the CATACT beamline at the KIT Light Source[16]. This beamline has a double crystal Si(111) monochromator and provides high intensity X-rays with energy resolution $E/\Delta E > 1\times10^4$ at the Co K-edge energy. The spectra of the three Co complexes and two reference compounds CoO and Co_2O_3 were recorded at the K-edge of cobalt. The energy was calibrated to the tabulated value of the Co K-edge energy (7709 eV) measured as the energy of the first peak in the first derivative spectrum of Co metal foil and which corresponds to the major inflection point in the Co K-edge. The samples were in the form of pellets, which were prepared of the mixture of calculated amount of finely powdered complex/compound and appropriate amount of cellulose (as binder) for yielding an edge step of absorbance 1.0 across the Co K-edge.[17]

Software packages *Athena* and *Artemis*[18] were used for the analysis of EXAFS data by following procedures similar to that outlined in ref. [17]. The theoretical model was generated using the available crystallographic data[74] of analogous complex **4**. The model was fitted to the experimental data of all the three complexes **1-3** in k-space and R-space to obtain the local structural parameters around the Co absorbing atom. Peak fitting module available in Demeter[18] has been used for calculating the intensity of pre-edge peak present in the complexes.

Software *FEFF9*[19] has been used to perform ab-initio calculations to simulate XANES spectra at the K edge of cobalt and to obtain ℓ-density of state (DOS), ℓ being orbital angular momentum, in complexes **1-3** by following procedures similar to that outlined in ref. [17]. These calculations, which are based on real-space full multiple scattering approach, enable deeper insight into the electronic nature of the Co centres in the complexes. By using the crystal structure data of **4**, atoms input file has been generated which is used to create the feff input file for performing ab initio XANES simulations.In the present calculations, Hedine-Lundqvist potential, XANES, SCF, FMS and Absolute cards were used. The LDOS card was added for calculation of density of states.

3. Results and discussions

3.1 Energy dispersive X-ray Spectroscopy (EDX)

EDX spectra provided information about the elemental composition of the complexes **1**-**3**. Figs. 2(a) and (b) show the EDX spots and EDX spectrum for complex **1**, respectively. The average atomic and weight percentage composition of the elements as obtained by averaging values determined from different spots on the sample surfaces are listed in table form. The analysis shows the presence of Co, C, O, N and Na with a Na/Co ratio of about 1:8. Corresponding EDX results for complexes **2** and **3** are given in supporting information, Figs. S1 and S2, respectively.

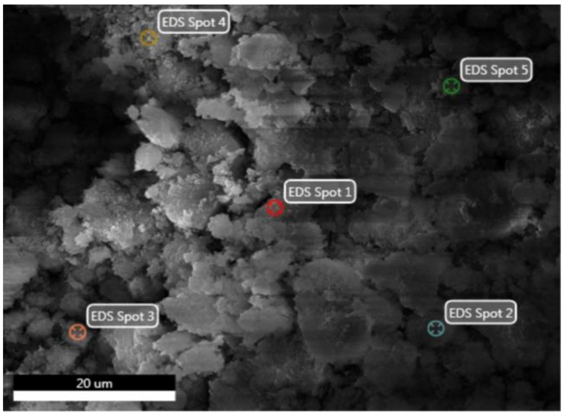

Fig. 2(a). EDX spots of $Na[Co_8\{O_2CCH_3\}_8(OCH_3)_{16}]NO_3$ (**1**)

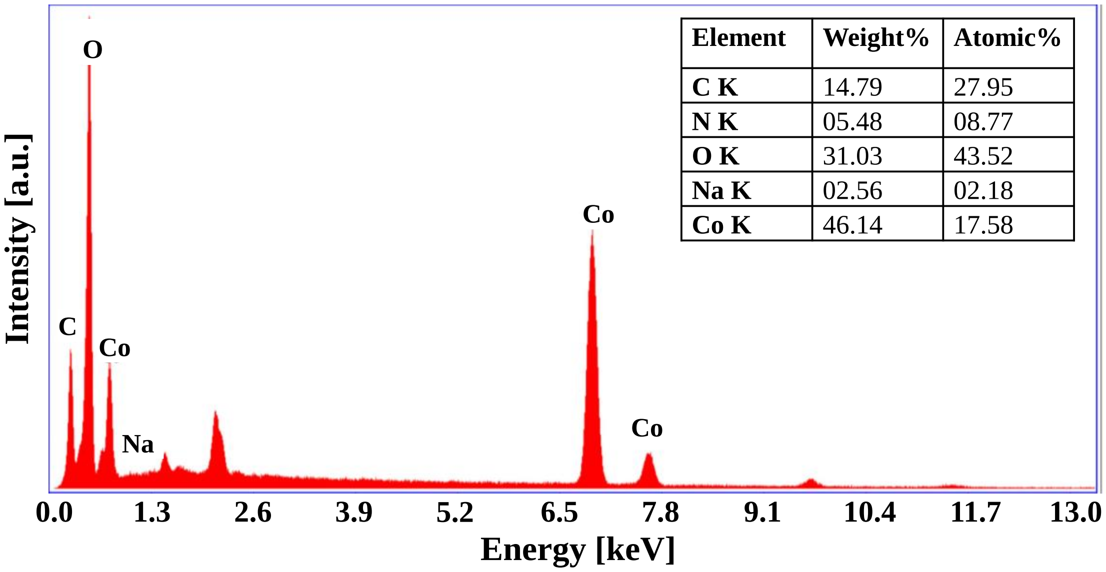

Element	Weight%	Atomic%
C K	14.79	27.95
N K	05.48	08.77
O K	31.03	43.52
Na K	02.56	02.18
Co K	46.14	17.58

Fig 2(b). EDX spectrum of $Na[Co_8\{O_2CCH_3\}_8(OCH_3)_{16}]NO_3$ (**1**) and the averaged weight% and atomic % values of the elements determined from different spots on the sample surfaces as shown in Fig 1(a).

3.2 XANES interpretation

Fig. 3(a) shows the Co K-edge XANES spectra of the complexes **1-3** and of the reference compounds Co_2O_3 and CoO. In these complexes, the shift in the Co K-edge with respect to that in the Co metal edge (~7709 eV), i.e., chemical shift is analyzed by comparing it with that of the CoO and Co_2O_3 for estimation of the oxidation state of central absorbing Co atoms. First derivative XANES spectra for the complexes are given in supporting information, Fig. S3. Complex **1** shows comparatively lower chemical shift compared to **2** and **3** indicating higher contribution from Co^{2+} ions in this complex. On the other hand, chemical shift for **2** and **3** was observed on higher energy indicating +3 oxidation state of Co ions in these complexes.

Pre-edge peak P, which occurs just before the Co K-edge, is shown separately in Fig. 3(b). It has been observed with higher intensity in Co_2O_3 and with very low intensity in CoO. In an ideal octahedral symmetry, this feature is an electric dipole forbidden transition but in tetrahedral environments, due to the lack of the inversion centre, the transition is allowed[20-24]. In higher oxidation states, the metal–ligand (O/N) bond-lengths shorten, resulting in higher mixing of p and d orbitals and increase in the intensity of this peak. The pre-edge peak in complexes **1-3** is seen clearly at ~ 7710 eV in Fig.3(b). The difference in the nature of pre-edge feature present in the complexes has been quantitatively determined by peak fitting module available in *Demeter*[18]. The fitting has been done using a pseudo-Voigt (pvoigt) profile and results are given in supporting information, Fig. S4. Based on the results of peak fitting analysis, the intensity of pre-edge peak has the order **2** > **3** ≈ **1**. Hence, Co ions present in **2** show strong Co^{3+} nature as compared to **1** and **3**.

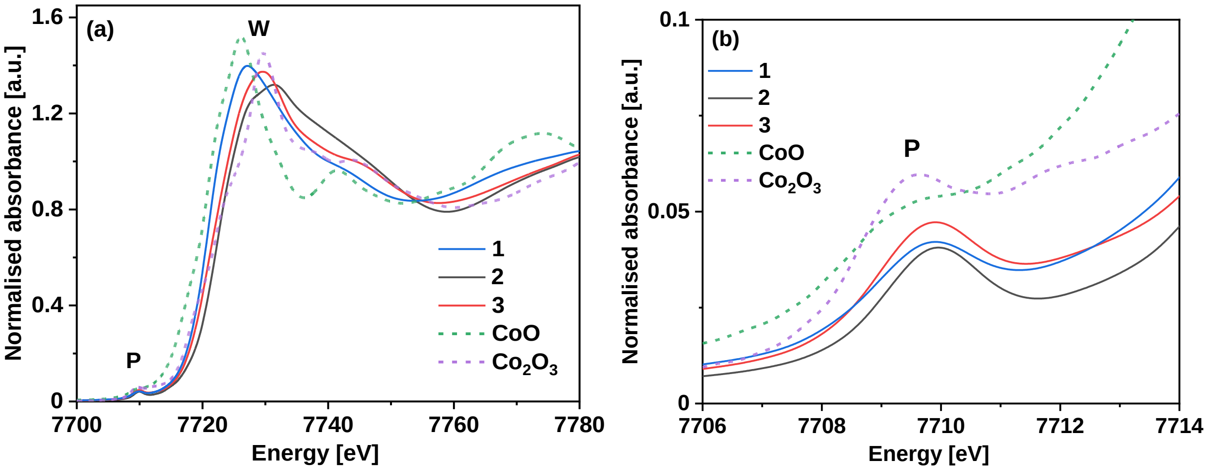

Fig 3. (a) XANES spectra at the Co K-edge for the complexes **1-3.** Spectra of the standards CoO and Co_2O_3 are also shown for comparison. (b) Peak P shown in pre-edge region.

Another important characteristic feature for oxidation state is the white line feature W, observed at ~ 7729 eV for Co^{3+}(Co_2O_3) and at ~ 7726 eV for Co^{2+}(CoO). This feature is assigned the transition 1s→ 4p (unoccupied) in Co, which is dipole allowed in both octahedral and tetrahedral coordinated Co atoms[23, 25-27]. For complex **1**, this feature is observed at ~ 7726.7 eV indicating presence of Co^{2+}. The feature is observed at ~ 7730 eV and 7729 eV for complexes **2** and **3**, respectively, indicating presence of Co^{3+}. Also, in case of **2** slight splitting of this feature is observed. Based on chemical shift and white line feature, +2 as well as +3 oxidation state can be assigned to Co centers in **1** and +3 oxidation state to Co centres in **2** and **3**.

3.3 EXAFS analysis

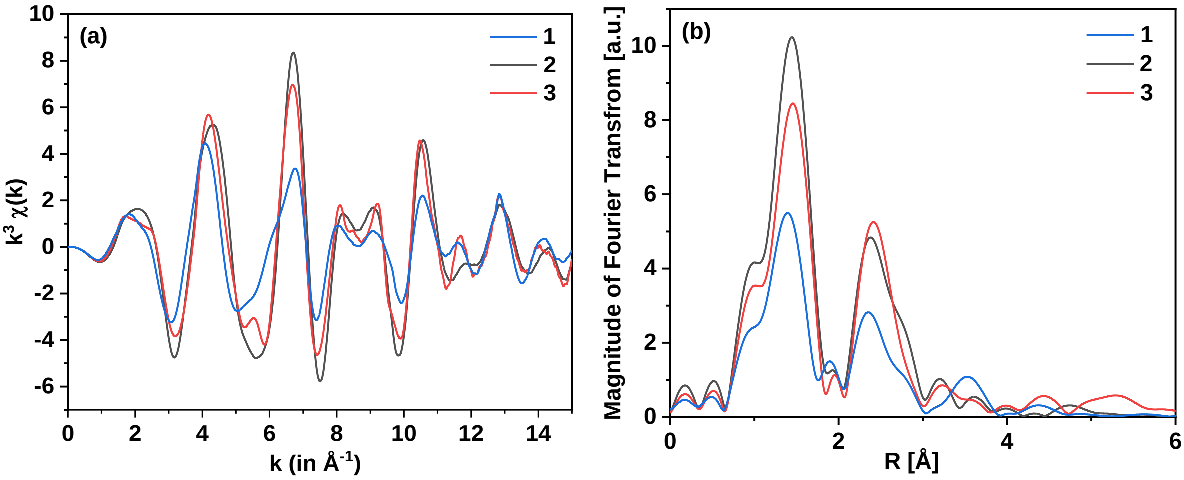

Fig 4(a). k^2weighted χ(k) vs. k EXAFS spectra of complexes **1-3**, (b) Corresponding Fourier transformed spectra in R-space.

Fig. 4(a) shows the k^2 weighted χ(k) EXAFS spectra for complexes **1-3**. As seen in the figure, the oscillations are similar in the three complexes indicating identical local environment of Co atoms in the complexes. Fig. 4(b) shows the corresponding Fourier transform in R-space, in which the position and amplitude of the peaks, representing the different shells around the absorbing Co atom, are seen to be similar in the three complexes.

The theoretical model generated using the crystallographic data available for complex **4**, which is analogous to the complexes **1-3**, has been fitted to the experimental data of the complexes **1-3.** Fitting has been done both in R-space (range 1.0 – 4 Å) and in k-space (range 2.4 - 12.5 $Å^{-1}$) using k weight of 3. The fitting and the contribution of different paths are shown in R-space in Figs. 5(a-c). Table 1 gives the local structure parameters around Co atom obtained as a result of the fitting.

As seen from table 1, the distances of the six oxygen atoms around the absorbing Co atom are in the range of ~ 1.89-1.93 Å in complexes **1-3**. The CoO_6 distorted octahedra is formed by oxygen atoms O1, O2, O4 and O7 in the square plane and O3 and O6 in axial positions. The local structure around Co centres as determined from the analysis of EXAFS thus confirm that the Co atom has octahedral coordination in the complexes **1-3**. In the higher shells, two more Co atoms are observed at distances 2.76 and 2.77 Å in **1**, 2.81 and 2.82 Å in **2**, and at 2.82 and 2.83 Å in **3**. Thus, in **1** the Co atoms are observed at lower distance than in **2** and **3**. Also, it can be observed from R factor values that theoretical model generated using crystal structure of **4** fits much better to the experimental data of **2** (R value = 0.00017) and **3** (R value = 0.00022) as compared to that of **1** (R value = 0.00121).

Table 1. Local structure parameters obtained as a result of fitting of theoretical model to experimental data.

	Complex **1**				Complex **2**			Complex **3**		
	S_0^2 = 0.74, ΔE_0 = -6.8(2.0) eV R factor= 0.00121				S_0^2 =0.87 , ΔE_0 = 0.90(1.26) eV R factor=0.00017			S_0^2 = 0.75 ΔE_0 = 0.75 (1.26) eV R factor= 0.00022		
	N	R(Å)	R_c(Å)	σ^2x10^3 (Å^2)	N	R(Å)	σ^2x10^3 (Å^2)	N	R(Å)	σ^2x10^3 (Å^2)
O1	1	1.89(0.01)	1.88	10.7(1.9)	1	1.89(0.01)	5.6(0.7)	1	1.90(0.02)	6.3(0.7)
O2	1	1.90(0.01)	1.89	10.7(1.9)	1	1.90(0.01)	5.6(0.7)	1	1.90(0.02)	6.3(0.7)
O3	1	1.90(0.01)	1.89	10.7(1.9)	1	1.90(0.01)	5.6(0.7)	1	1.90(0.02)	6.3(0.7)
O7	1	1.90(0.01)	1.90	10.7(1.9)	1	1.90(0.01)	5.6(0.7)	1	1.91(0.02)	6.3(0.7)
O4	1	1.91(0.01)	1.91	10.7(1.9)	1	1.91(0.01)	5.6(0.7)	1	1.92(0.02)	6.3(0.7)
O6	1	1.93(0.01)	1.92	10.7(1.9)	1	1.92(0.01)	5.6(0.7)	1	1.93(0.02)	6.3(0.7)
Co1'	1	2.76(0.10)	2.86	5.4(1.5)	1	2.81(0.05)	5.5(0.7)	1	2.82(0.04)	4.3(0.7)
Co2	1	2.77(0.10)	2.87	5.4(1.5)	1	2.82(0.05)	5.5(0.7)	1	2.83(0.04)	4.3(0.7)
R = Bond distance obtained from EXAFS analysis, R_c= Crystallographic value of bond distance in complex **4**, N = coordination number, σ^2= Debye-Waller factor. 'R factor' is parameter showing goodness of fit. The error bars are given in parenthesis.										

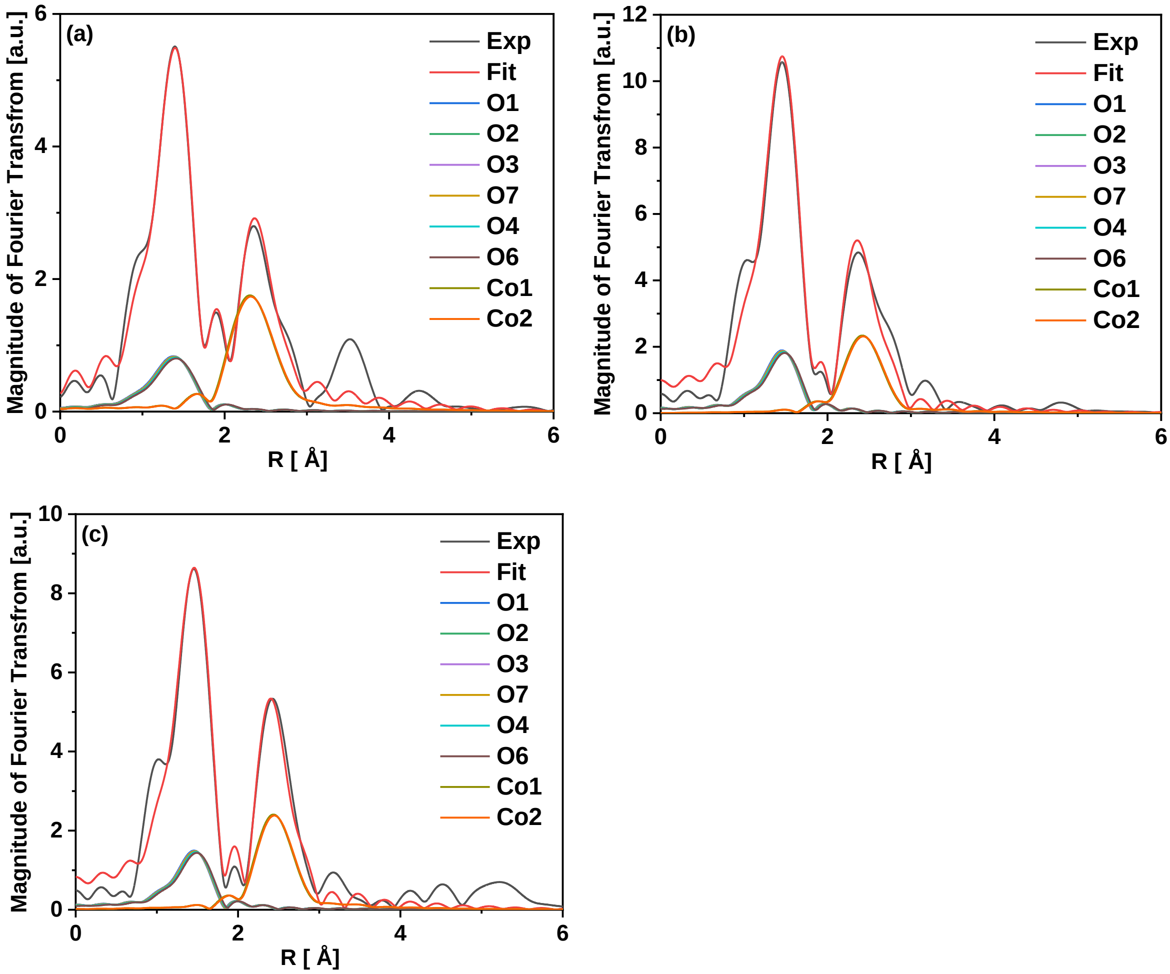

Fig.5. EXAFS fittings, in R-space, for the complexes **1-3** shown in Figs.(a)-(c) respectively. The experimental curve is shown by black line and the theoretical fit by red line. The contributions of the different paths are also shown in the figures.

Following Beattie et al[7], the results obtained from EXAFS analysis can be interpreted to yield the molecular structure of complexes **1-3** which is depicted in Fig. 6. The Co atoms Co1, Co1' and Co2 are three of the eight Co atoms which are seen to be at the vertices of a near regular planar octagon and which give toroidal shape to the molecule.

The results obtained for complexes **1-3** from EXAFS analysis indicate that the coordination environment of Co centers in complexes **1-3** should be similar to that of the complex **4.** To further investigate the structure, XANES has been analyzed in the following section 3.4.

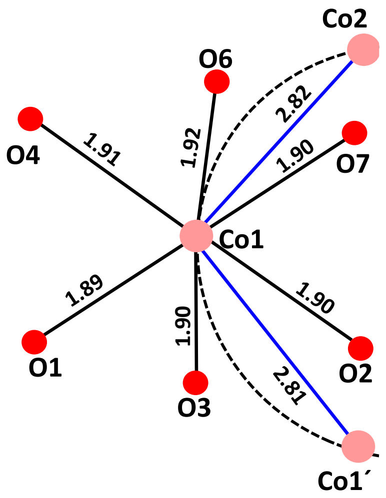

Fig 6. Local structure around Co1 centre in complex **1** as determined from the analysis of EXAFS. The CoO_6 distorted octahedra is formed by Co atoms O1,O2,O4 and O7 in the square plane and O3 and O6 in axial positions. The Co atoms Co1, Co1' and Co2 are three of the eight Co atoms which are at the vertices of a near regular planar octagon and which give toroidal shape to the molecule. Bond distances shown are in Å.

3.4 Ab-initio XANES calculations

According to Beattie et al.[7], the shape of the analogous complex **4** is highly symmetric toroidal. The four $[Co_2(\mu\text{-}MeCO_2)(\mu\text{-}OMe)_2]$ units form the eight edge-shared CoO_6 distorted octahedra. At the vertices of a near regular planar octagon are the eight cobalt atoms. We have simulated the XANES spectra for these eight Co centres of complex **4** using software *FEFF9*. For simulating the XANES spectra, the core hole has been set at the eight different positions of Co atom, namely, Co1, Co2, Co3, Co4, Co1', Co2', Co3' and Co4', in order to compare their electronic structure. Since the four atoms Co1, Co2, Co3, Co4, are symmetrical to the other four atoms Co1', Co2', Co3' and Co4', simulations have been shown only for the four Co atoms. The XANES spectra, simulated by *FEFF9*, for the four positions of the Co centres in complex **4** are given in all the three Figs.7(a), (b) and (c). It can be seen in any of these figures that the features of the simulated spectra for centres Co3 and Co4 are nearly the same, for centre Co2, they are slightly different and for centre Co1, the difference is strong. The theoretically simulated spectra for the four Co centres have been merged to get the resultant simulated spectrum, which is also shown in the three figures. The merged spectrum has been obtained by merging all the simulated spectra for the four centres by taking equal contribution from each spectrum. To compare the simulated spectrum with the experimental spectrum of the complexes **1**, **2** and **3**, the latter spectra are also included in Figs.7(a), (b) and (c) respectively. The theoretical and experimental spectra shown in these three figures are aligned by *Athena*.

The features and shape of simulated XANES spectra for different positions can be easily compared with the experimentally measured spectra of complexes. In Fig 7(a), the experimental spectrum of **1** has features close to that of Co2 position (as shown by arrow) indicating higher contribution from such Co centres. Similarly, in Fig 7(b), the XANES features of **2** resemble more to that of features of Co1 position (as shown by arrow). In case of **3** (Fig 7 (c)), XANES features are closer to that of Co3 and Co4 positions. Thus, it can be deduced from these comparisons that the presence of different ligands around the octanuclear ring present in these complexes causes variation in the electronic structure of Co centres as observed from the difference in their XANES features.

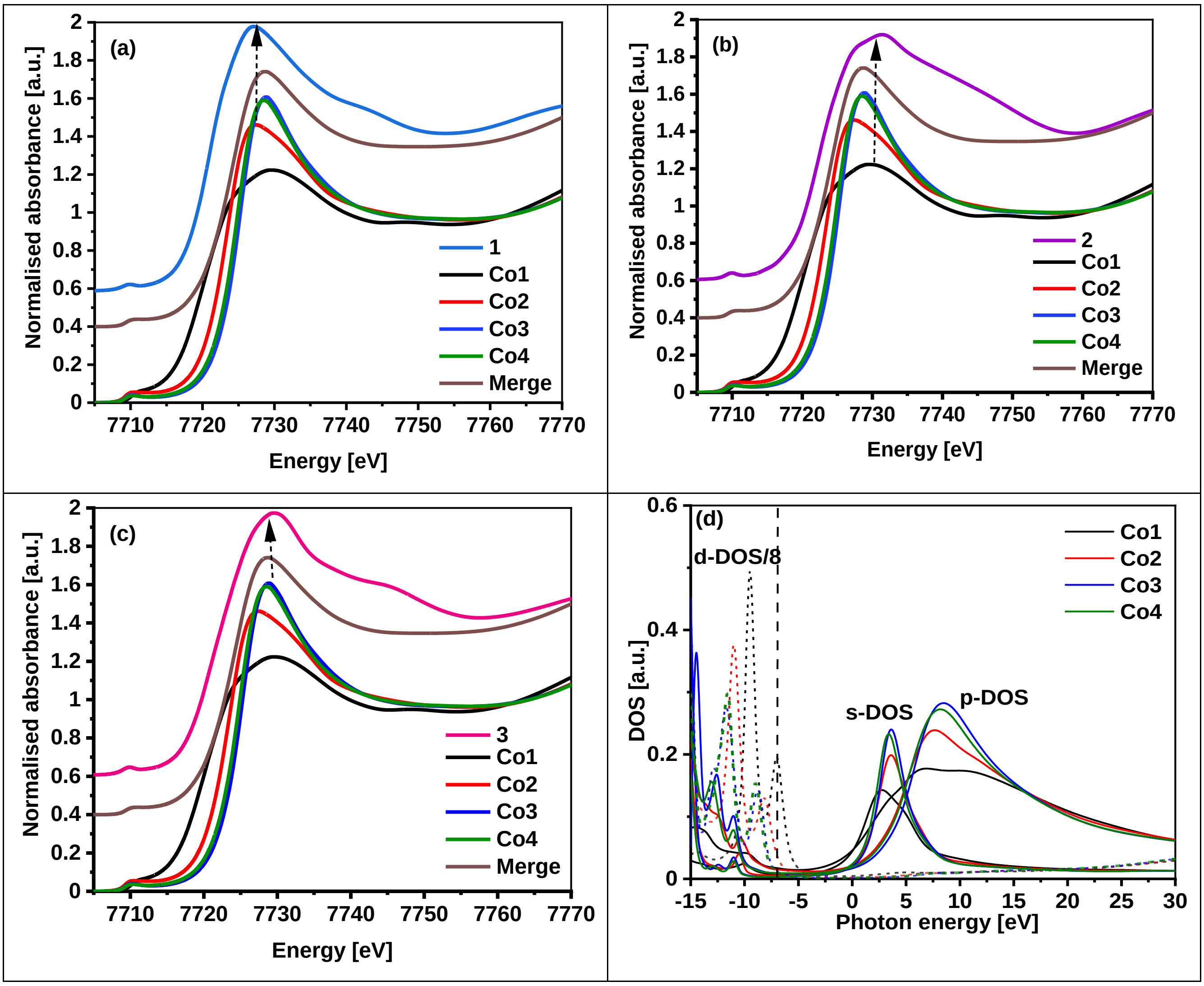

Fig 7. Simulated XANES spectra obtained by setting in the calculations, the core hole at four of the eight Co centres, Co1, Co2, Co3, Co4 for Co atoms situated at the vertices of a nearly regular planar octagon. The spectra for the complexes **1-3** are shown in the figs. (a)-(c) respectively. The theoretically simulated spectra for the four Co centre have been merged to get the resultant spectrum are also shown in the figures. (d) Corresponding s- and p-DOS calculated simultaneously for Co centre at positions Co1, Co2, Co3 and Co4. The energy scale in this figure is relative to the energy E_0 of the absorption edge. The position of Fermi level is shown by a vertical dashed line.

The simulated XANES spectra for the four Co centres show the pre-edge peak at ~7710 eV. The peak is observed well resolved for Co centres present at positions Co2, Co3 and Co4 indicating oxidation state of +3 for Co with distorted octahedral coordination. However, for Co1 centre, the pre-edge peak is very weak indicating the oxidation state lower than +3 for this Co centre. Also, the value of edge shift for Co1 position is found to be lower than that found for the other three Co positions Co2, Co3 and Co4. This observation indicates that there should be comparatively lower charge on metal ion at Co1 position in comparison to the other three positions. Further, at Co1 position, the intensity of white line feature is quite low and shows broadening. For Co3 and Co4 positions the white line is intense and shows no broadening. The features of the white line at Co2 position have mixed nature. All these observations of the differences in the XANES features show that the Co ions present at Co1 position have different electronic structure as compared to the other three positions.

As these XANES features are strongly correlated to the density of states of Co, the corresponding s- and p- and d-DOS have also been calculated simultaneously when the simulated XANES spectra for complex **4** were obtained using *FEFF9*. The DOS curves for the four positions Co1, Co2, Co3 and Co4 are shown in the Fig. 7(d). It is worth mentioning here that the DOS distribution as obtained from *FEFF9* shown here does not resolve principal quantum number, and gives a sum of 1s, 2s, 3s etc. However, in most cases the DOS near the fermi level is dominated by a particular principal quantum number for each angular momentum. Hence, in the present case of Co as central absorbing atom, all of the d-DOS near the Fermi level (shown by vertical dashed line in the figure) was for 3d, and the s- and p- DOS were form 4s and 4p.

For Co1 (black line), the p-DOS maximum which corresponds to white line feature in XANES spectrum has broad distribution in the region from 5eV to 15 eV which explains broad and less intense nature of white line. s-DOS also has fair contribution in the region from 0-10 eV indicating mixing of s and p orbitals in the edge region. For Co2, p-DOS distribution has a maximum followed by slight hump which is in line with the appearance of corresponding white line. s-DOS distribution in this case is slightly shifted towards higher energy as compared to that of Co1. In case of Co3 and Co4, p-DOS has clear maximum with comparatively higher intensity which correlates well with the intense white line observed in their simulated XANES spectrum. For these Co centres, s-DOS distributions were shifted towards higher energy and have higher contribution in the edge region. In the energy region from -15eV to -5eV which corresponds to pre-edge region in XANES, the d-DOS distribution for Co1 appears to be uniform (unaffected) whereas for other three Co centres d-DOS were observed with lower intensity and broad distribution indicating participation of d orbitals (mostly 3d) in the bond formation with the ligands.

Hence, it has been shown that the Co centres situated at the vertices of an octagon have distinct electronic structure due to the interaction of ligands with Co at these positions as observed from the corresponding DOS distributions.

4. Conclusions

The electronic structure of octanuclear cobalt complexes **1**-**3** have been investigated by analysing both XANES and EXAFS and by theoretically simulating the XANES spectra. For complex **1**, a weak pre-edge feature, comparatively lower edge-shift and presence of white line feature at ~ 7727 eV point towards mixed nature of Co centres, i.e., Co^{2+}/ Co^{3+}. In case of complexes **2** and **3**, well resolved pre-edge feature, edge shift closer to Co_2O_3 and white line feature at ~ 7729 eV indicate Co^{3+} nature of Co centres. EXAFS analysis confirmed the local structure around Co centers in complexes **1-3,** where Co is surrounded by six oxygen atoms in the range of ~ 1.89-1.93 Å forming the distorted octahedra. Co-Co backscattering at ~ 2.76 Å in **1** and at ~ 2.82 Å in **2** and **3** shows the presence of three of the eight Co atoms situated at the vertices of a nearly regular planar octagon. XANES simulations performed by setting the core hole at four different positions of octagon showed that Co ions present at Co1 position has different electronic structure, i.e., broadening of white line and weak pre-edge feature, as compared to the other three positions. Corresponding DOS curves calculated simultaneously for these sites were found to correlate well to their XANES features. p-DOS has broad distribution for Co1 centre, whereas Gaussian distribution with single maximum for other three centres. Hence by using simulated XANES spectra, it has been shown that the Co centres situated at the vertices of an octagon in octanuclear Co complexes have distinct electronic structures due to the interaction with ligands which in turn, affects the DOS distribution leading to different features in XANES.

Acknowledgement

We would like to thank the Institute for Beam Physics and Technology (IBPT) for the operation of the storage ring, the Karlsruhe Research Accelerator (KARA)

References

1. Kostakis, G. E.; Perlepes, S. P.; Blatov, V. A.; Proserpio, D. M.; Powell, A. K., High-nuclearity cobalt coordination clusters: Synthetic, topological and magnetic aspects. *Coordination Chemistry Reviews* **2012,** *256* (11), 1246-1278.

2. Liu, W.; Sahoo, B.; Junge, K.; Beller, M., Cobalt Complexes as an Emerging Class of Catalysts for Homogeneous Hydrogenations. *Accounts of Chemical Research* **2018,** *51* (8), 1858-1869.

3. Chakrabarty, R.; Bora, S. J.; Das, B. K., Synthesis, Structure, Spectral and Electrochemical Properties, and Catalytic Use of Cobalt(III)−Oxo Cubane Clusters. *Inorganic Chemistry* **2007,** *46* (22), 9450-9462.

4. Dimitrou, K.; Sun, J.-S.; Folting, K.; Christou, G., The [Co4O4]4+ Cubane as a Quadruply-Bridging Unit: The Mixed-Valence Cluster [Co8O4(O2CPh)12(solv)4] (solv = DMF, MeCN, H2O). *Inorganic Chemistry* **1995,** *34* (16), 4160-4166.

5. Beattie, J. K.; Hambley, T. W.; Klepetko, J. A.; Masters, A. F.; Turner, P., The chemistry of cobalt acetate—IV. The isolation and crystal structure of the symmetric cubane, tetrakis[(μ-acetato)(μ3-oxo)(pyridine)cobalt(III)] · chloroform solvate, [Co4(μ3-O)4(μ-CH3CO2)4(C5H5N)in4] · 5CHCl3 and of the dicationic partial cubane, trimeric, [(μ-acetato)(acetato)tris(μ-hdyroxy(μ3-oxo) hexakispyridinetricobalt(III)]hexafluorophosphate · water solvate, [Co3(μ3-O)(μ-OH)3(μ-CH3CO2(CH3CO2(C5H5N)6[PF6]2 · 2H2O. *Polyhedron* **1998,** *17* (8), 1343-1354.

6. Dimitrou, K.; Folting, K.; Streib, W. E.; Christou, G., Lewis basicity of the [Co4O4]4+ cubane core. Preparation of a mixed-valence (4Co, 4Co) cluster with an unusual [Co8(μ4-O)4]2+ core, and new [Co4O3(OH)]5+ and [Co4O2(OH)2]6+ cubane complexes. *Journal of the Chemical Society, Chemical Communications* **1994,** (11), 1385-1386.

7. Beattie, J. K.; Hambley, T. W.; Klepetko, J. A.; Turner, P., Supramolecular self-assembly of a toroidal inclusion complex, [NH4][Co8(MeCO2)8(OMe)16][PF6]. *Chemical Communications* **1998,** (1), 45-46.

8. Brechin, E. K.; Cador, O.; Caneschi, A.; Cadiou, C.; Harris, S. G.; Parsons, S.; Vonci, M.; Winpenny, R. E. P., Synthetic and magnetic studies of a dodecanuclear cobalt wheel. *Chemical Communications* **2002,** (17), 1860-1861.

9. Fursova, E.; Kuznetsova, O.; Ovcharenko, V.; Romanenko, G.; Ikorskii, V.; Eremenko, I.; Sidorov, A., Simultaneous transformation of a polynuclear complex and nitroxide in the reaction of the {Co6(O)2Piv10} cluster with 2,4,4,5,5-pentamethyl-4,5-dihydro-1H-imidazolyl-(3-oxide)-1-oxyl. *Polyhedron* **2007,** *26* (9), 2079-2088.

10. Lapshin, A. E.; Magdysyuk, O. V., Structure of a catalytically active octanuclear cobalt complex [Co(II)4Co(III)4(μ4-O)4(μ-O2CPh)12(PhCOOH)4]. *Glass Physics and Chemistry* **2011,** *37* (3), 307-315.

11. Russell, M. E.; Hawes, C. S.; Ferguson, A.; Polson, M. I. J.; Chilton, N. F.; Moubaraki, B.; Murray, K. S.; Kruger, P. E., Synthesis, structural and magnetic characterisation of iron(ii/iii), cobalt(ii) and copper(ii) cluster complexes of the polytopic ligand: N-(2-pyridyl)-3-carboxypropanamide. *Dalton Transactions* **2013,** *42* (37), 13576-13583.

12. Holmberg, R. J.; Kay, M.; Korobkov, I.; Kadantsev, E.; Boyd, P. G.; Aharen, T.; Desgreniers, S.; Woo, T. K.; Murugesu, M., An unprecedented CoII cuboctahedron as the secondary building unit in a Co-based metal–organic framework. *Chemical Communications* **2014,** *50* (40), 5333-5335.

13. Argent, S. P.; Tarassova, I.; Greenaway, A.; Nowell, H.; Barnett, S. A.; Warren, M. R.; Tang, C. C.; Morris, C. G.; Lewis, W.; Champness, N. R.; Schröder, M.; Blake, A. J., Assembly of high nuclearity clusters from a family of tripodal tris-carboxylate ligands. *Polyhedron* **2016,** *120*, 18-29.

14. Radu, I.; Kravtsov, V. C.; Ostrovsky, S. M.; Reu, O. S.; Krämer, K.; Decurtins, S.; Liu, S.-X.; Klokishner, S. I.; Baca, S. G., Tetranuclear {CoII2CoIII2}, Octanuclear {CoII4CoIII4}, and Hexanuclear {CoIII3DyIII3} Pivalate Clusters: Synthesis, Magnetic Characterization, and Theoretical Modeling. *Inorganic Chemistry* **2017,** *56* (5), 2662-2676.

15. Alexandropoulos, D. I.; Dolinar, B. S.; Xie, H.; Vignesh, K. R.; Dunbar, K. R., A Co8 metallacycle stabilized by double anion–π interactions. *Chemical Communications* **2019,** *55* (82), 12356-12359.

16. Zimina, A.; Dardenne, K.; Denecke, M. A.; Doronkin, D. E.; Huttel, E.; Lichtenberg, H.; Mangold, S.; Pruessmann, T.; Rothe, J.; Spangenberg, T.; Steininger, R.; Vitova, T.; Geckeis, H.; Grunwaldt, J.-D., CAT-ACT—A new highly versatile x-ray spectroscopy beamline for catalysis and radionuclide science at the KIT synchrotron light facility ANKA. *Review of Scientific Instruments* **2017,** *88* (11), 113113.

17. Gaur, A.; Sharma, D.; Nitin Nair, N.; Mehta, B. K.; Shrivastava, B. D.; Gogoi, M.; Sarmah, N.; Das, B. K., Investigating cubane formation and effect of co-crystallization agents in oxo-bridged Co complexes using X-ray absorption spectroscopy. *Journal of Molecular Structure* **2021,** *1244*, 130869.

18. Ravel, B.; Newville, M., ATHENA, ARTEMIS, HEPHAESTUS: data analysis for X-ray absorption spectroscopy using IFEFFIT. *Journal of Synchrotron Radiation* **2005,** *12* (4), 537-541.

19. Rehr, J. J.; Kas, J. J.; Vila, F. D.; Prange, M. P.; Jorissen, K., Parameter-free calculations of X-ray spectra with FEFF9. *Physical Chemistry Chemical Physics* **2010,** *12* (21), 5503-5513.

20. Adak, S.; Hartl, M.; Daemen, L.; Fohtung, E.; Nakotte, H., Study of oxidation states of the transition metals in a series of Prussian blue analogs using x-ray absorption near edge structure (XANES) spectroscopy. *Journal of Electron Spectroscopy and Related Phenomena* **2017,** *214*, 8-19.

21. Choi, H. C.; Lee, S. Y.; Kim, S. B.; Kim, M. G.; Lee, M. K.; Shin, H. J.; Lee, J. S., Local Structural Characterization for Electrochemical Insertion−Extraction of Lithium into CoO with X-ray Absorption Spectroscopy. *The Journal of Physical Chemistry B* **2002,** *106* (36), 9252-9260.

22. de Groot, F.; Vankó, G.; Glatzel, P., The 1s x-ray absorption pre-edge structures in transition metal oxides. *Journal of Physics: Condensed Matter* **2009,** *21* (10), 104207.

23. Jacobs, G.; Chaney, J. A.; Patterson, P. M.; Das, T. K.; Davis, B. H., Fischer–Tropsch synthesis: study of the promotion of Re on the reduction property of Co/Al2O3 catalysts by in situ EXAFS/XANES of Co K and Re LIII edges and XPS. *Applied Catalysis A: General* **2004,** *264* (2), 203-212.

24. Jacobs, G.; Patterson, P. M.; Zhang, Y.; Das, T.; Li, J.; Davis, B. H., Fischer–Tropsch synthesis: deactivation of noble metal-promoted Co/Al2O3 catalysts. *Applied Catalysis A: General* **2002,** *233* (1), 215-226.

25. Chadwick, A. V.; Savin, S. L. P.; Fiddy, S.; Alcántara, R.; Fernández Lisbona, D.; Lavela, P.; Ortiz, G. F.; Tirado, J. L., Formation and Oxidation of Nanosized Metal Particles by Electrochemical Reaction of Li and Na with NiCo2O4: X-ray Absorption Spectroscopic Study. *The Journal of Physical Chemistry C* **2007,** *111* (12), 4636-4642.

26. Kim, K.-S.; Lee, Y.-K., Technical Communication. *International Journal of Hydrogen Energy* **2010,** *35* (11), 5378-5382.

27. Rønning, M.; Tsakoumis, N. E.; Voronov, A.; Johnsen, R. E.; Norby, P.; van Beek, W.; Borg, Ø.; Rytter, E.; Holmen, A., Combined XRD and XANES studies of a Re-promoted Co/γ-Al2O3 catalyst at Fischer–Tropsch synthesis conditions. *Catalysis Today* **2010,** *155* (3), 289-295.

Supporting information

Probing the electronic nature of Co centers forming the planar ring in octa-nuclear Co complexes using X-ray absorption spectroscopy

Nirupamjit Sarmah[1], Deepa Sharma[2], B.K.Mehta[2], B.D.Shrivastava[3], B.K.Das[1], A. Zimina[4,5], A.Gaur[4,5*]

[1]*Department of Chemistry, Gauhati University, Guwahati 781 014, India*
[2]*School of Studies in Chemistry and Bio-chemistry, Vikram University, Ujjain 456010, India*
[3]*School of Studies in Physics, Vikram University, Ujjain 456010, India*
[4]*Institute of Catalysis Research and Technology (IKFT), Karlsruhe Institute of Technology, Eggenstein-Leopoldshafen 76344, Germany*
[5]*Institute for Chemical Technology and Polymer Chemistry (ITCP), Karlsruhe Institute of Technology, Karlsruhe 76131, Germany*

**Corresponding author: abhijeet.gaur@kit.edu, abhijeetgaur9@gmail.com*

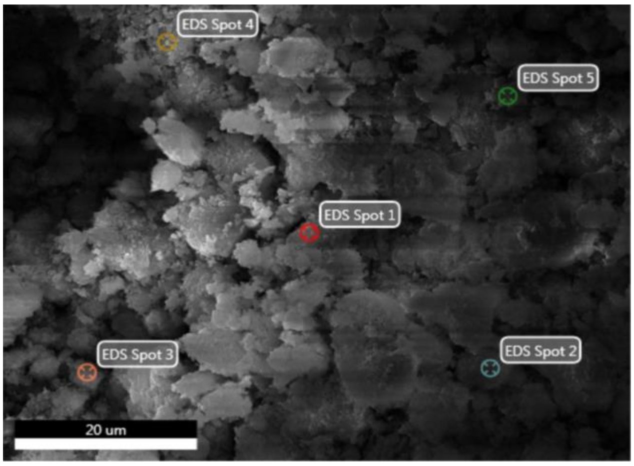

Figure S1(a). EDX spot of $Na[Co_8\{O_2CC(CH_3)_3\}_8(OCH_3)_{16}]NO_3$ (**2**)

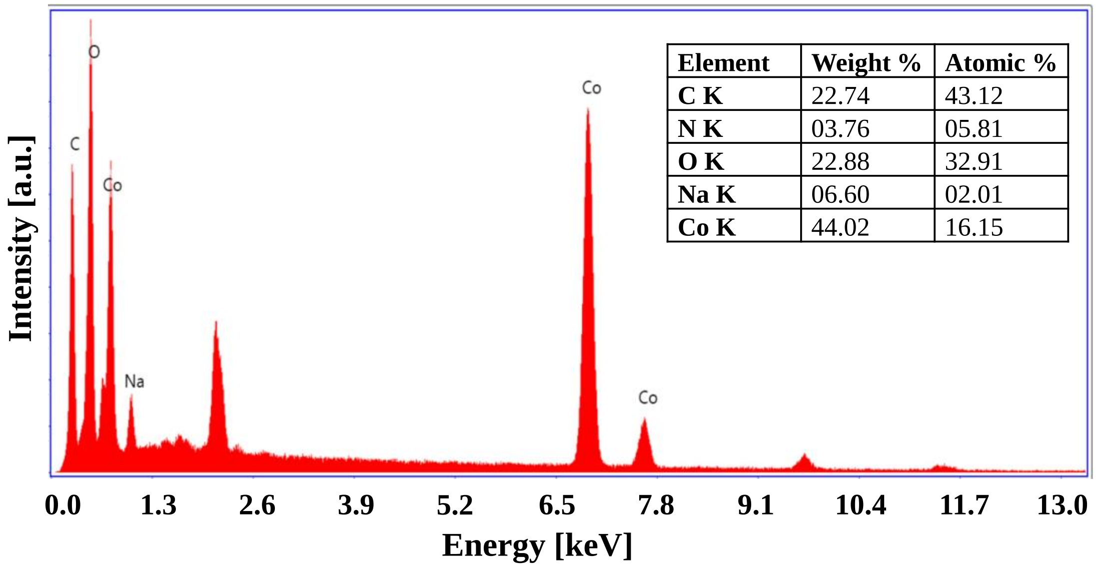

Element	**Weight %**	**Atomic %**
C K	22.74	43.12
N K	03.76	05.81
O K	22.88	32.91
Na K	06.60	02.01
Co K	44.02	16.15

Figure S1(b). EDX spectrum of $Na[Co_8\{O_2CC(CH_3)_3\}_8(OCH_3)_{16}]NO_3$ (**2**) and the averaged weight% and atomic % values of the elements determined from different spots on the sample surfaces as shown in Fig S1(a).

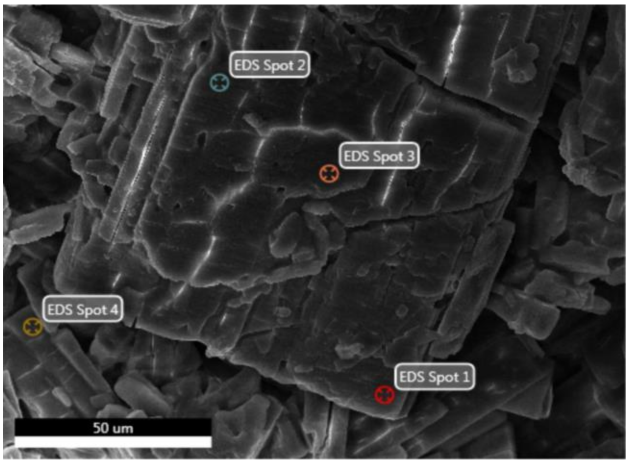

Figure S2(a). EDX spot of Na[$Co_8\{O_2CC(CH_3)_3\}_8(OC_2H_5)_{16}$]$NO_3$ (**3**)

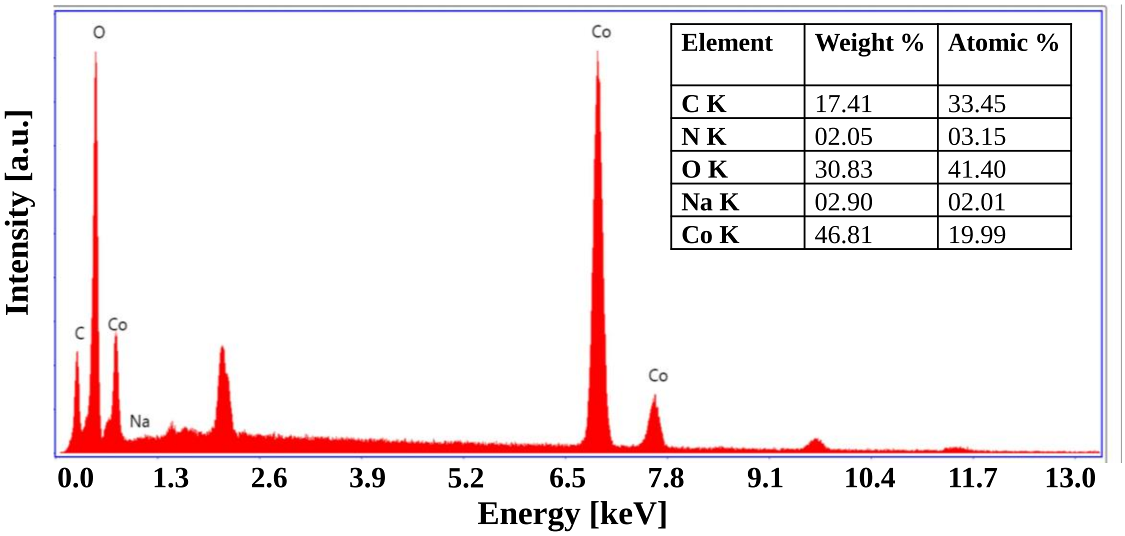

Element	**Weight %**	**Atomic %**
C K	17.41	33.45
N K	02.05	03.15
O K	30.83	41.40
Na K	02.90	02.01
Co K	46.81	19.99

Figure S2(b). EDX spectra Na[$Co_8\{O_2CC(CH_3)_3\}_8(OC_2H_5)_{16}$]$NO_3$ (**3**) and the averaged weight% and atomic % values of the elements determined from different spots on the sample surfaces as shown in Fig S2(a).

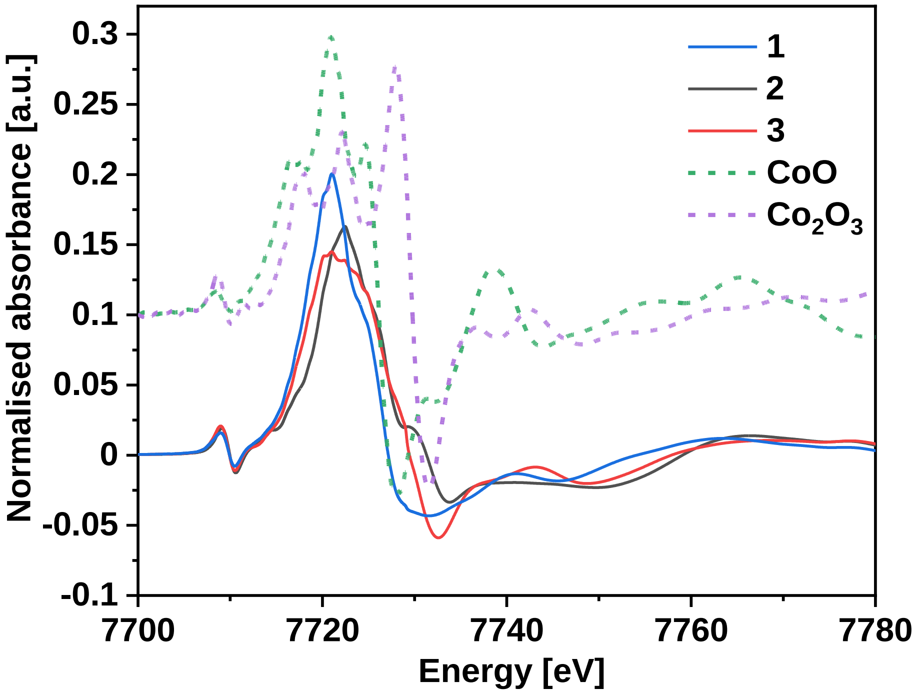

Fig.S3. Co K-edge derivative XANES spectra for complexes **1-3.** Derivative spectra of the standards CoO and Co_2O_3 are also shown for comparison.

(a) Complex **1**

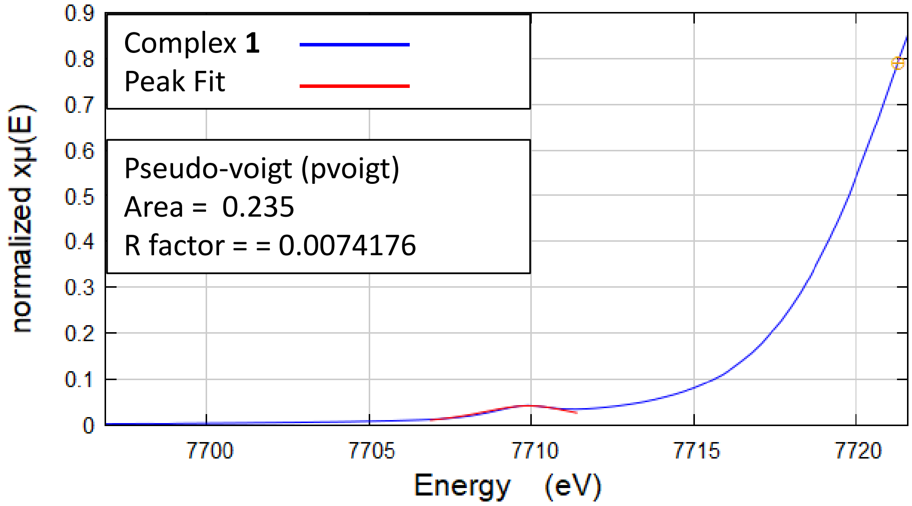

(b) Complex **2**

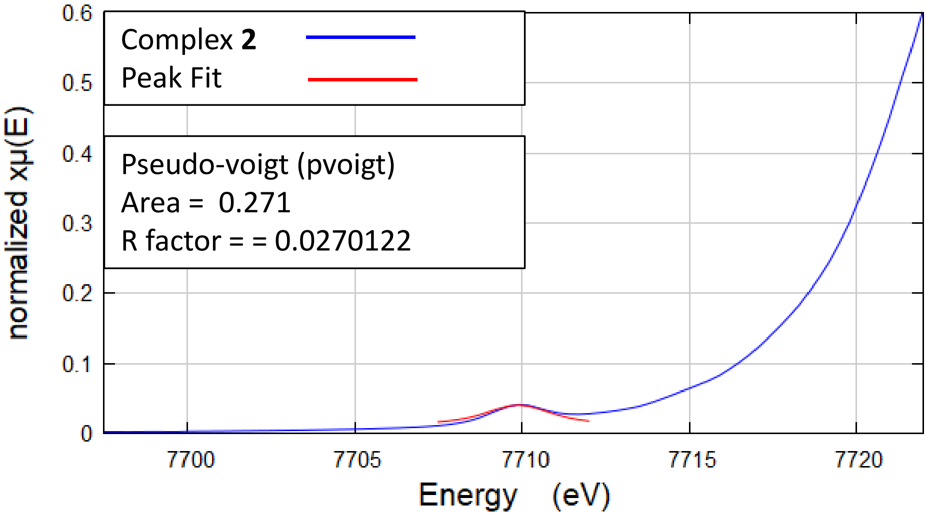

(c) Complex **3**

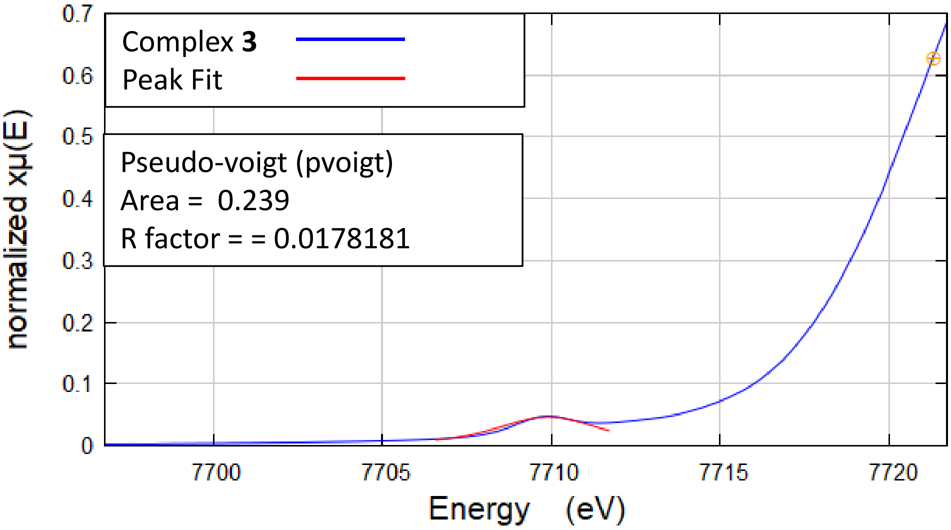

Fig. S4 Pre-edge peak fitting curves as obtained from Demeter and corresponding fitting results for the complexes.